Journal of Power Sources 195 (2010) 8189–8193

Contents lists available at ScienceDirect

Journal of Power Sources

journal homepage: www.elsevier.com/locate/jpowsour

Short communication

Fabrication of a carbon nanofiber sheet as a micro-porous layer for proton exchange membrane fuel cells

Qiongjuan Duan [b], Biao Wang [a,b,*], Jiong Wang [b], Huaping Wang [a,b], Yonggen Lu [b]

[a] State Key Laboratory for Modification of Chemical Fibers and Polymer Materials, Donghua University, Shanghai 201620, PR China
[b] College of Material Science and Engineering, Donghua University, Shanghai 201620, PR China

ARTICLE INFO

Article history:
Received 28 May 2010
Received in revised form 13 July 2010
Accepted 13 July 2010
Available online 17 July 2010

Keywords:
Micro-porous layer
Carbon nanofiber sheet
Gas diffusion layer
Proton exchange membrane fuel cell
Electrospinning

ABSTRACT

A carbon nanofiber sheet (CNFS) has been prepared by electrospinning, stabilisation and subsequent carbonisation processes. Imaging with scanning electron microscope (SEM) indicates that the CNFS is formed by nonwoven nanofibers with diameters between 400 and 700 nm. The CNFS, with its three-dimensional pores, shows excellent electrical conductivity and hydrophobicity. In addition, it is found that the CNFS can be successfully applied as a micro-porous layer (MPL) in the cathode gas diffusion layer (GDL) of a proton exchange membrane fuel cell (PEMFC). The GDL with the CNFS as a MPL has higher gas permeability than a conventional GDL. Moreover, the resultant cathode GDL exhibits excellent fuel cell performance with a higher peak power density than that of a cathode GDL fabricated with a conventional MPL under the same test condition.

1. Introduction

Proton exchange membrane fuel cells (PEMFCs) have recently attracted considerable interest as alternative renewable power sources for various applications due to their high efficiency, environmental benefits and low operating temperature [1–3]. However, the low operating temperature poses a particularly serious problem because it allows excess water to exist, inside the PEMFC, which increases the mass transport limitations in the fuel cell. It is generally believed that the continuous generation of water in the cathode gas diffusion layer (GDL) during the operation of the fuel cell causes the cathode to flood, which reduces the oxygen diffusion rate to the cathode catalyst layer, leading to a degradation of the fuel cell performance [4,5]. Therefore, the management of liquid water is crucial in achieving good performance and efficient operation of the PEMFC. Most techniques for liquid water management focus on excess water removal to prevent the catalyst layer from flooding under humidified conditions and maintaining full hydration of the electrolyte membrane with high proton conductivity under sub-saturated conditions [6]. Unfortunately, the best strategy for water management in PEMFC is not fully understood [4].

The GDL, which is located between the bipolar plate and catalyst layer, is widely regarded as the most critical PEMFC component for water management. To manage water and achieve efficient gas transport, the GDL is usually made hydrophobic by treatment with a fluoropolymer dispersion [7–9]. In addition, a micro-porous layer (MPL) consisting of carbon particles mixed with a fluoropolymer dispersion is also applied to promote the effective removal of liquid water from the cathode catalyst layer into the GDL [10–13]. Various types of carbon materials with different microstructures have been investigated to improve the water management capabilities of MPLs and thus improve PEMFC performance. Wang et al. developed a novel MPL with a different amount of Acetylene Black and Black Pearls 2000 carbon and found that the structure of the novel MPL could enhance the transport of both liquid water and reactant gases in the fuel cell [10,11]. Carbon nanofibers and nanotubes were adopted in an MPL for the first time in Park et al.'s publication [12]. The experimental results demonstrated that the adoption of carbon nanomaterials improved the gas permeability and electric conductivity of the MPL. Hung et al. also added vapour-grown carbon nanofibers into the carbon black/PTFE MPL. The maximum power density obtained using the prepared MPL during the single cell test was around 270 mWcm^{-2}, approximately 85% that of the ELAT GDL (commercial GDL) [14]. A further improvement was implemented by Kannan et al.'s group, who grew carbon nanotubes directly on carbon paper without a hydrophobic agent, and the resultant GDL showed very stable performance [15].

Even though many publications address carbon nanomaterials in MPLs, the application of a carbonised electrospun nanofiber sheet

* Corresponding author at: College of Material Science and Engineering, Donghua University, 2999, North Renmin Road, Shanghai 201620, PR China
Tel.: +86 21 67792731; fax: +86 21 67792855.
E-mail address: wbiao2000@dhu.edu.cn (B. Wang).

0378-7753/$ – see front matter © 2010 Elsevier B.V. All rights reserved.
doi:10.1016/j.jpowsour.2010.07.032

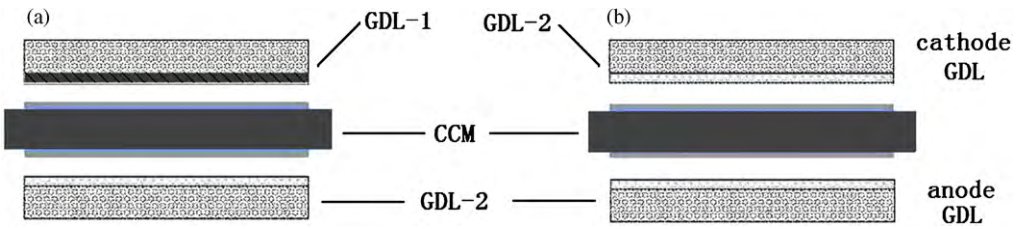

Fig. 1. Schematic diagram of the MEA samples: (a) MEA-1 and (b) MEA-2.

as possible MPL has not yet been fully exploited for fuel cell applications.

The electrospinning technique is a highly versatile method to process solutions or melts into an interconnected membrane-like web of superfine fibers with diameters ranging from a few nanometers to several micrometers. Because of the large surface areas and small pore size, nonwoven sheets composed of electospun fibers have become excellent candidates in many applications [16–18]. It is worth mentioning that the development of carbon nanofibers using a combination of the electrospinning technique and subsequent thermal treatments is easier and costs less than other processes for making carbon nanofibers [19,20]. In this study, a carbon nanofiber sheet (CNFS) has been prepared by electrospinning and subsequent thermal treatments. The structure and properties of the CNFS have been characterised and the single cell performance using CNFS as MPL has also been tested.

2. Experimental

2.1. Preparation of CNFS

The CNFS was fabricated via electrospinning and subsequent thermal treatments. A polyacrylonitrile (PAN, Aldrich) nanofiber sheet was obtained by electrospinning. The PAN solution, with a concentration of 8 wt.% in Dimethylacetamide (DMAc, Aldrich) was prepared at 60 °C with mechanical stirring for 36 h. The solution was loaded into a 5 mL syringe with a capillary tip with a diameter of 0.9 mm. The flow rate of the polymer solution was 1 mL h^{-1} and was controlled by a syringe pump. A variable high voltage power supply was used to provide a potential difference of 14 kV. The collector plate was made of carbon sheet and the tip-to-collector distance was 15 cm. The as-spun PAN nanofiber sheet was later converted into a CNFS by stabilising at 250 °C for 2 h in air with a heating rate of 5 °C min^{-1} and carbonising at 900 °C for 2 h with a heating rate of 3 °C min^{-1} in nitrogen.

2.2. Characterisation of nanofiber sheets

X-ray diffraction (XRD) patterns of the nanofiber sheets were recorded using a Rigaku D/Max 2550 VB/PC X-ray diffractometer with Cu Kα radiation (λ = 0.15418 nm) for diffraction angles 2θ spanning 5–60°. The electrical resistance of the CNFS was measured by the four-probe technique using Keithley 6517 Resistance Meters. The contact angle (CA) of a water droplet was determined using an optical video contact angle instrument (OCA 40, Dataphysics, Germany) to estimate the wettability of the nanofiber sheets. The CA measurement was taken after the water droplet maintaining on the surface of the samples for 10 s. The morphology of the CNFS was evaluated using a scanning electron microscope (SEM, JSM-5600LV, JEOL, Japan).

2.3. Preparation of GDLs with different MPLs

Two different GDLs were prepared using different MPLs. GDL-1 was obtained by hot pressing carbon fiber paper (P50T, Ballard Applied Materials) with the above prepared CNFS at 150 °C under a pressure of 3 MPa for 3 min, while GDL-2 was made with carbon fiber paper and a conventional MPL. A slurry of Vulcan XC-72R carbon powder (Cabot Corp.) and 40 wt.% Teflon FEP 121A (DuPont Co., Ltd.) suspension was stirred for 30 min at room temperature and then coated on the carbon fiber paper by blade coating to fabricate the conventional MPL with a carbon loading of 1 mg cm^{-2}. Heat treatment was subsequently performed by baking the MPL-coated GDL at 120 °C for 15 min and then sintering at 350 °C for 15 min.

The gas permeability characteristics for GDL-1 and GDL-2 were evaluated using a Gurley Apparatus (Model 4110). The GDLs were held between clamping plates having a circular orifice. The test measures the time required for 300 cc of air to flow through an area of 0.25 $in.^2$ (1.61 cm^2) of the sample tested, under a light uniform pressure of 12.4 cm water. The electrical resistance of the GDLs was also measured by four-probe technique using Keithley 6517 Resistance Meters.

2.4. MEA preparation and cell performance test

A Pt/C catalyst (40 wt.%, Johnson Matthey Corp.) was used as the catalyst for both the anode and cathode, and a Nafion 212 membrane (DuPont Co., Ltd.) was used as the electrolyte membrane. To prepare the catalyst layer, a homogeneous suspension was formed from the Pt/C catalyst and Nafion solution (Aldrich, 5 wt.% Nafion) with an isopropanol mixture as a solvent. The weight ratio of Pt/C to the solid content of Nafion in the solution was 2:1. The resulting slurry was deposited onto a Nafion 212 membrane by a spraying procedure (thickness about 40 μm). The platinum loading was 0.4 mg cm^{-2} for both the anode and cathode. Finally, the samples were dried at 70 °C for 30 min. Nafion solution was used as the ionic component to strengthen the three-dimensional reaction zone of the electrodes [21].

The schematic of the MEA samples is shown in Fig. 1. MEA-1 was prepared by hot pressing the catalyst-coated Nafion 212 membrane (CCM) between the GDL-2 (anode) and GDL-1 (cathode) at 160 °C under a pressure of 3 MPa for 90 s. MEA-2 was prepared in the same way as MEA-1 except that GDL-2 was used for both anode and cathode.

The MEAs were then put inside a single cell test station (with 5 cm^2 of active area) for evaluation of cell performance. The test station was equipped with temperature controllers and humidification bottles. The single cell performance was evaluated by measuring the cell voltage as a function of the current density at 70 °C with H_2/air as reactant gas under ambient pressure. The relative humidity of the H_2 and air was maintained at 100%. Three identical MEAs for each sample were tested to measure the repeatability of the experiments.

3. Results and discussion

The CNFS was prepared from an electrospun PAN nanofiber sheet by heat treatment including stabilisation and carbonisation. Fig. 2 shows the X-ray diffraction patterns of the PAN nanofiber sheet (a) as-spun, (b) after stabilisation and (c) after carbonisa-

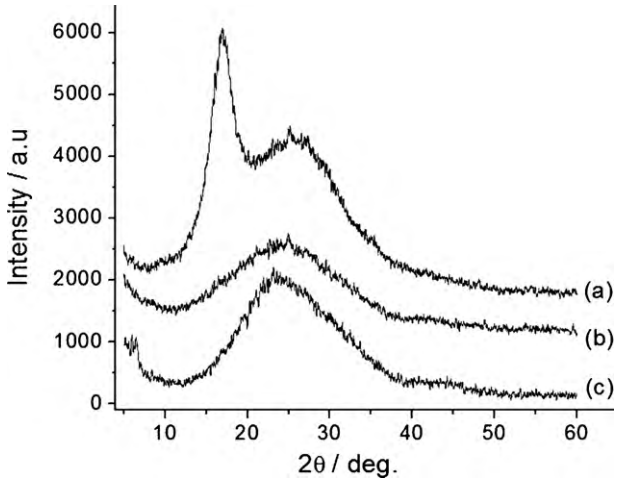

Fig. 2. XRD patterns of a prepared electrospun PAN-based nanofiber sheet: (a) as-spun, (b) after stabilisation and (c) carbonisation.

tion. A very strong diffraction peak at $2\theta = 17^\circ$ appears in Fig. 2a, which reflects the (1 0 0) plane of a hexagonal structure and corresponds to a planar spacing $d = 5.240$ Å. There is another relatively weak diffraction peak with a value of 2θ at 29° corresponding to the $d = 3.04$ Å from the (1 1 0) reflections [22]. The diffraction pattern of the samples after stabilisation shows a wide and weak peak at $2\theta = 25.5^\circ$ (Fig. 3b), which relates to the ladder polymer structure, and the peaks around 17° and 29° have completely disappeared. As can be seen from Fig. 3c, the diffraction peak around $2\theta = 25.5$ strengthened after carbonisation, demonstrating the formation of a turbostratic graphite structure [23]. The transformation of PAN-based nanofibers to turbostratic carbon nanofibers leads to an electrically conductive nanofiber sheet. The in-plane resistivity of the CNFS determined from the four-probe technique was 15.83 mΩ cm, which means that the CNFS meets the electrical requirements of a MPL in the fuel cell.

Fig. 3 shows the morphological microstructures of the CNFS. As can be seen from Fig. 3, the diameters of the carbon nanofibers range from 400 to 700 nm and the CNFS has a porous morphology with a three-dimensional interconnected structure. Hence, the microstructure of the CNFS could improve the gas permeability and water removal in the cathode when the CNFS is applied to the GDL as a possible MPL.

The wetting behaviour of a solid can be determined by a CA measurement of a water droplet on the surface. In the process of measuring the water CA on the nanofiber sheets, we found that the PAN nanofiber sheet and the stabilised nanofiber sheet exhibited contact angles of 0°. This phenomenon may be attributed to the polar PAN nature and the formation of –OH and –COOH during the stabilisation treatment of PAN in air. However, after carbonisation, the carbon nanofiber sheets were hydrophobic, and the average water contact angle of the carbon nanofiber sheets was around 136° as shown in Fig. 4. This may result from the volatilisation of non-carbon element from the nanofiber in the form of methane, water, carbon dioxide and other gases. The results of the CA measurements also revealed that the carbon nanofiber sheets lower their surface energy after carbonisation without any modification by materials of low surface energy.

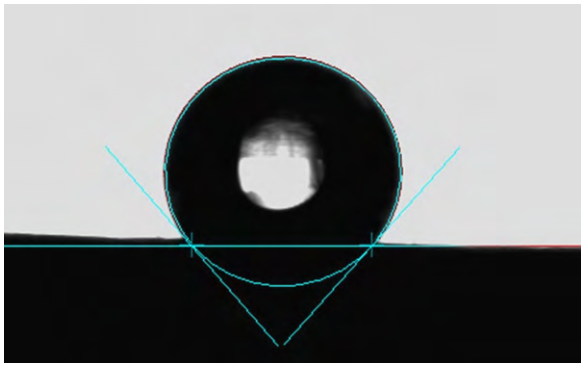

Fig. 4. Photographs of a static water droplet on the surface of a CNFS.

Fig. 5 shows the SEM photographs of the surface and a cross-section of the GDL with different kinds of MPLs. The surface microstructure of the CNFS MPL (Fig. 5a) illustrates a porous nanofiber membrane. Compared with conventional MPL fabricated with carbon powder and FEP (Fig. 5c), the CNFS showed three-dimensional pores favouring reactant gases transport. In the case of conventional MPL, carbon powder is uniformly distributed on the carbon fiber paper without large cracks which may lead to a limited reactant gas diffusion rate. As seen from Fig. 5b and d, the CNFS MPL presented a uniform thickness of around 25 μm, while the conventional MPL presented a non-uniform thickness between 15 and 30 μm. Parts of the carbon powder in the conventional MPL had fallen into the pores of the carbon fiber paper, blocking the way of reactant gases. By contrast, the CNFS MPL was connected to the carbon fiber paper with the pores in the carbon fiber paper unblocked. This may decrease the hindrance for the reactant gas flow from the flow channels to the catalyst layer [24].

The gas permeability estimated from the Gurley device was 45.44 $cm^3\ cm^{-2}\ s^{-1}$ for GDL-1 and 29.57 $cm^3\ cm^{-2}\ s^{-1}$ for GDL-2. This result implies that GDL-1 has double the gas permeability of GDL-2. However, the electrical resistance test of both GDLs showed similar resistances of approximately 12 mΩ cm., and this may have resulted from the carbon fiber paper substrate, which is the dominant factor in the electrical conductivity of the GDLs.

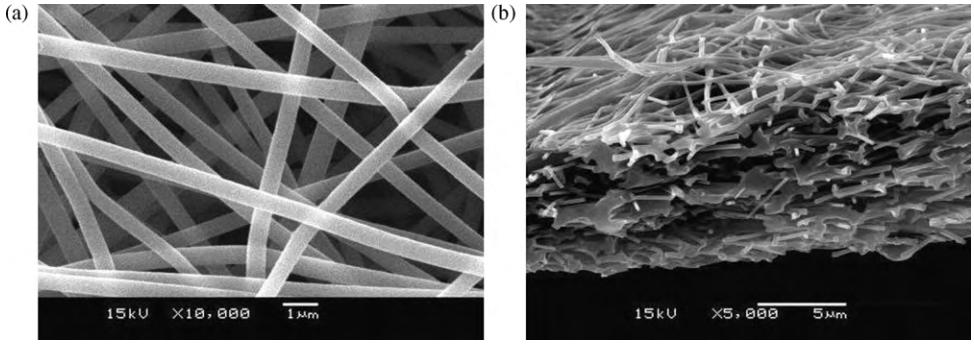

Fig. 3. SEM images of the surface (a) and cross-section (b) of a CNFS.

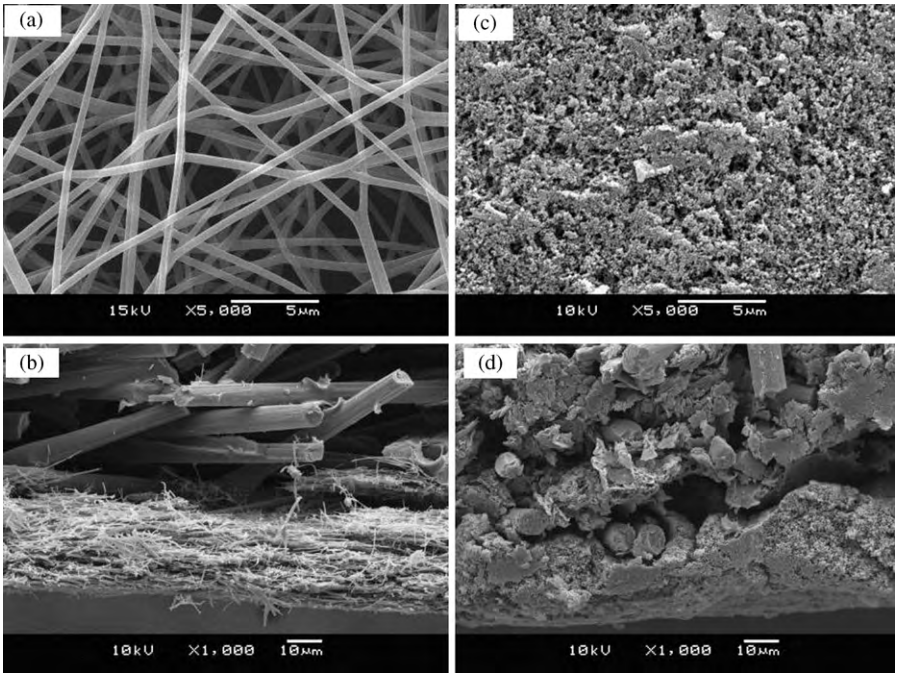

Fig. 5. SEM micrographs of the top-view and cross-section images of MEA-1 (a and b) and MEA-2 (c and d).

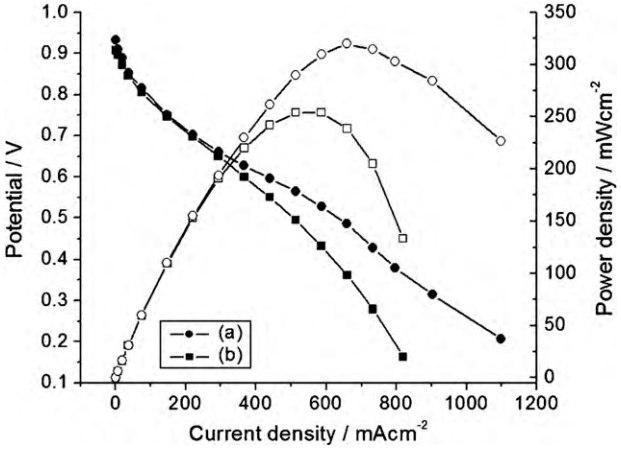

Fig. 6. Fuel cell performance of MEAs: (a) MPL-1 and (b) MEA-2.

The single cell performances for the prepared MEAs at 70 °C using air and H_2 as reactant gases are presented in Fig. 6. It was found that the maximum power density of the GDL fabricated with a CNFS MPL was 321 mW m^{-2}, which was about 23% higher than that of the conventional GDL. This result can be attributed to the hydrophobic properties and better gas transport path of the CNFS MPL in the PEMFC.

4. Conclusions

A CNFS was successfully prepared by means of electrospinning and subsequent thermal treatments. It was formed by nonwoven nanofibers with diameters between 400 and 700 nm, and it exhibited excellent electrical conductivity, gas permeability and hydrophobicity. The CNFS MPL exhibited a homogeneous carbon nanofiber distribution and a crack-free surface morphology with a structure of three-dimensional pores favouring gas transport. The fuel cell performance of the resultant MEAs was evaluated using a fuel cell test station at 70 °C in an H_2/air system. It is worth pointing out that the maximum power density of MEA-1 (with the CNFS as the MPL in the cathode GDL) was 321 mW cm^{-2}, which was around 23% higher than that of MEA-2 (with the conventional MPL in the cathode GDL) under the same testing conditions.

Acknowledgments

This work was financially supported by the Natural Science Foundation of Shanghai, China (No. 09ZR1401500), the Scientific Research Foundation for the Returned Overseas Chinese Scholars (Ministry of Education), the Cultivating Project of the Key Laboratory of High Performance Fibers and Products (Donghua University Ministry of Education), Shanghai Leading Academic Discipline Project (B603) and Program of Introducing Talents of Discipline to Universities (No. 111-2-04).

References

[1] S. Litster, G. McLean, J. Power Sources 130 (2004) 61–76.
[2] A.D.J. Larminie, Fuel Cell Systems Explained, John Wiley and Sons, Chichester, 2000.
[3] C.Y. Wang, Chem. Rev. 104 (2004) 4727–4765.
[4] L. Cindrella, A.M. Kannan, J.F. Lin, K. Saminathan, Y. Ho, C.W. Lin, J. Wertz, J. Power Sources 194 (2009) 146–160.
[5] J.T. Gostick, M.A. Ioannidis, M.W. Fowler, M.D. Pritzker, Electrochem. Commun. 11 (2009) 576–579.
[6] J.H. Jiang, A. Kucernak, J. Electroanal. Chem. 567 (2004) 123–137.
[7] S.B. Park, S. Kim, Y. Park, M.H. Oh, J. Phys: Conf. Ser. 165 (2009) 012046.
[8] G. Velayutham, J. Kaushik, N. Rajalakshmi, K.S. Dhathathreyan, Fuel Cells 7 (2007) 314–318.
[9] G.G. Park, Y.J. Sohn, T.H. Yang, Y.G. Yoon, W.Y. Lee, C.S. Kim, J. Power Sources 131 (2004) 182–187.
[10] X.L. Wang, H.M. Zhang, J.L. Zhang, H.F. Xu, X.B. Zhu, J. Chen, B.L. Yi, J. Power Sources 162 (2006) 474–479.
[11] X.L. Wang, H.M. Zhang, J.L. Zhang, H.F. Xu, Z.Q. Tian, J. Chen, H.X. Zhong, Y.M. Liang, B.L. Yi, Electrochim. Acta 51 (2006) 4909–4915.
[12] G.G. Park, Y.J. Sohn, S.D. Yim, T.H. Yang, Y.G. Yoon, W.Y. Lee, K. Eguchi, C.S. Kim, J. Power Sources 163 (2006) 113–118.
[13] A.M. Kannan, L. Munukutla, J. Power Sources 167 (2007) 330–335.
[14] T.F. Hung, J. Huang, H.J. Chuang, S.H. Bai, Y.J. Lai, Y.W. Chen-Yang, J. Power Sources 184 (2008) 165–171.
[15] A.M. Kannan, P. Kanagala, V. Veedu, J. Power Sources 192 (2009) 297–303.
[16] J.H. Park, Y.W. Ju, S.H. Park, H.R. Jung, K.S. Yang, W.J. Lee, J. Appl. Electrochem. 39 (2009) 1229–1236.

[17] N.N. Bui, B.H. Kim, K.S. Yang, M.E. Dela Cruz, J.P. Ferraris, Carbon 47 (2009) 2538–2539.
[18] L. Zou, L. Gan, F.Y. Kang, M.X. Wang, W.C. Shen, Z.H. Huang, J. Power Sources 195 (2010) 1216–1220.
[19] C. Hsu, H. Lee, C. Lin, C. Lee, Metall. Mater. Trans. A 41A (2010) 768–774.
[20] H. Lee, H. Yoon, G. Kim, Appl. Phys. A: Mater. 97 (2009) 559–565.
[21] J.H. Lin, W.H. Chen, S.H. Su, Y.K. Liao, T.H. Ko, J. Power Sources 184 (2008) 38–43.
[22] M.J. Yu, Y.J. Bai, C.G. Wang, Y. Xu, P.Z. Guo, Mater. Lett. 61 (2007) 2292–2294.
[23] M. Jing, C.G. Wang, Y.J. Bai, B. Zhu, Y.X. Wang, Polym. Bull. 58 (2007) 541–551.
[24] A.M. Kannan, S. Sadananda, D. Parker, L. Munukutla, J. Wertz, M. Thommes, J. Power Sources 178 (2008) 231–237.